

# Classification of Magnetic Forces on Antiferromagnetic Domain Wall

H. Y. Yuan,<sup>1,\*</sup> Weiwei Wang,<sup>2,\*</sup> Man-Hong Yung,<sup>3,4,†</sup> and X. R. Wang<sup>5,6,‡</sup>

<sup>1</sup>*Department of Physics, Southern University of Science and Technology, Shenzhen 518055, Guangdong, China*

<sup>2</sup>*Department of Physics, Ningbo University, Ningbo 315211, China*

<sup>3</sup>*Institute for Quantum Science and Engineering and Department of Physics,  
Southern University of Science and Technology, Shenzhen, 518055, China*

<sup>4</sup>*Shenzhen Key Laboratory of Quantum Science and Engineering, Shenzhen, 518055, China*

<sup>5</sup>*Department of Physics, The Hong Kong University of Science and Technology, Clear Water Bay, Kowloon, Hong Kong*

<sup>6</sup>*HKUST Shenzhen Research Institute, Shenzhen 518057, China*

(Dated: April 6, 2024)

A major challenge in spintronics is to find an efficient means to manipulate antiferromagnet (AFM) states, which are inert relative to a uniform magnetic field, due to the vanishingly-small net magnetization. The question is, how does an AFM response to an inhomogeneous field? Here we address the problem through a complete classification of the magnetic forces on an AFM domain wall (DW), revealing the following physical properties: (i) the tiny net magnetization still responds to the field gradient. (ii) the Néel order is sensitive to the field difference between two sublattices. (iii) DW energy has a quadratic dependence on the magnetic field due to its noncollinear structure. Remarkably, the first two factors drive DW to the opposite directions in a nanowire, but the third effect tends to push the DW to the high field region. Consequently, the competition among these three forces can be applied to understand the seemingly-contradictory results on AFM motion in literature. Additionally, our results provide a new route for a speedy manipulating AFM DW; our numerical simulation indicated that for a synthetic antiferromagnet, the DW propagating speed can reach tens of kilometers per second, an order of magnitude higher than that driven by an electric current.

*Introduction.*— Antiferromagnets (AFMs), being promising for spintronics, have attracted much attention for research in recent years [1–20], due to the superior stability and terahertz spin dynamics. However, at the same time, the high stability of AFM also represents a problem for controlling AFM states. Various methods, including electric currents through spin-transfer torque [7], spin-orbit torque [12, 13], spin waves [21], and thermal gradients [14, 22–24] have been proposed to manipulate AFM states, and in particular domain wall (DW) dynamics. However, each of these proposals has its own limitations. For example, although the spin-orbit torque can drive a DW propagating at a speed of up to several kilometers per second and is free of Walker breakdown [12], its application is limited to metals with a broken inversion symmetry, which excludes a large number of normal AFMs. On the other hand, for thermally-driven DW motion, the underlying physical mechanism remains unclear. Overall, finding efficient ways to manipulate AFM states remains a fundamental problem and is of crucial importance for a variety of applications.

Remarkably, determination of the DW propagating direction has become a debate topic [25–27]. One recent observation [28] is that AFM DWs do have a non-zero magnetization; they can interact with a magnetic field through the Zeeman effect. Consequently, it was first predicted that the DW velocity should be anti-symmetric relative to the applied magnetic field. However, this prediction was later challenged by another theory [12], which proposed a quadratic Zeeman energy for an AFM DW; in this way, the field-dependence of DW velocity should

be symmetric in the field direction instead. So, which one is correct? In fact, our numerical atomistic simulations indicate that neither of these two predictions are consistent in general, which calls for a need for a further investigation.

In this paper, we thoughtfully study the AFM DW motion under inhomogeneous fields, where we classify three DW driving forces based on the following observations. (i) The net magnetization of an AFM DW interacts with the field gradient of the nearest unit-cells as reported in Ref. [28]. (ii) In each unit cell, the Néel order interacts with the magnetic-field difference between the two sublattices, where the spin-orbit field [12] can be regarded as a special case. Note that the these two forces (i) and (ii) have a linear dependence in, respectively, the field gradient among unit-cells and field difference within each unit-cell. Furthermore, they tend to cancel each other. Finally, (iii) AFM DW energy depends on the average magnetic field quadratically due to the non-collinear structures.

Overall, the moving direction of an AFM DW depends on the interplay of all three mechanisms. These results provide an explanation on why our numerical results indicating that DW velocity is neither symmetric nor asymmetric, resolving the apparent inconsistency between the results of Ref. [12] and [28]. In addition, our classification of the forces points to a solution to designing a spatial profile on the magnetic field that can potentially drive an AFM DW to an unprecedentedly-high speed.

*Theory.*— Let us start with a two-sublattice AFM uniaxial nanowire along the  $z$  axis as shown in Fig. 1(a).

The system is described by the following Hamiltonian,

$$\mathcal{H} = J \sum_{\langle i,j \rangle} \mathbf{S}_{ai} \cdot \mathbf{S}_{bj} - K_z \sum_i (\mathbf{S}_{ai,z}^2 + \mathbf{S}_{bi,z}^2) - \sum_i (\mathbf{S}_{ai} \cdot \mathbf{H}_a + \mathbf{S}_{bi} \cdot \mathbf{H}_b), \quad (1)$$

where  $\mathbf{S}_{ai}$  ( $\mathbf{S}_{bj}$ ) ( $|\mathbf{S}_{ai}| = |\mathbf{S}_{bj}| = S$ ) are the spins on sublattices  $a$  ( $b$ ).  $\langle i, j \rangle$  denotes the nearest-neighboring sites.  $\mathbf{H}_a$  and  $\mathbf{H}_b$  are respectively the external field on sublattices  $a$  and  $b$ . The first and second terms in Eq. (1) are the exchange energy (coefficient  $J > 0$ ) and anisotropy energy (coefficient  $K_z > 0$ ), respectively. The third term is the usual Zeeman energy.

In terms of the magnetization,  $\mathbf{m} \equiv (\mathbf{S}_{ai} + \mathbf{S}_{bi})/2S$ , and Néel order,  $\mathbf{n} \equiv (\mathbf{S}_{ai} - \mathbf{S}_{bi})/2S$ , the Hamiltonian density  $\mathcal{H}$  in the continuum limit is given by, [8, 28]

$$\mathcal{H} = \frac{a}{2} \mathbf{m}^2 + \frac{A}{2} (\partial_z \mathbf{n})^2 - \frac{K}{2} n_z^2 + L \mathbf{m} \cdot \partial_z \mathbf{n} - \mathbf{m} \cdot \mathbf{h} + \mathbf{n} \cdot \mathbf{g}, \quad (2)$$

where  $a \equiv 4JS^2$  and  $A \equiv d^2JS^2$  are, respectively, homogeneous and inhomogeneous exchange constants with  $d$  being the lattice constant.  $K = 4K_zS^2$ .  $\mathbf{h} \equiv (\mathbf{H}_a + \mathbf{H}_b)/2$  and  $\mathbf{g} \equiv (\mathbf{H}_a - \mathbf{H}_b)/2$  are, respectively, the average field (over a unit cell) and field difference on the two sublattices (in a unit-cell). The term containing  $L \equiv 2dJS^2$  breaks the parity symmetry and results in a net magnetic moment of an AFM DW [28].

Consequently, the dynamics of the order parameters,  $\mathbf{m}$  and  $\mathbf{n}$ , are governed by the following equation of motion [7, 29],

$$\begin{aligned} \partial_t \mathbf{n} &= -\mathbf{n} \times (\mathbf{h}_m - \alpha_m \partial_t \mathbf{m}), \\ \partial_t \mathbf{m} &= -\mathbf{n} \times (\mathbf{h}_n - \alpha_n \partial_t \mathbf{n}) - \mathbf{m} \times (\mathbf{h}_m - \alpha_m \partial_t \mathbf{m}), \end{aligned} \quad (3)$$

where  $\mathbf{h}_m \equiv -\delta\mathcal{H}/\delta\mathbf{m}$  and  $\mathbf{h}_n \equiv -\delta\mathcal{H}/\delta\mathbf{n}$  are, respectively, the effective fields on the magnetization order  $\mathbf{m}$  and Néel order  $\mathbf{n}$ . One of the main contribution to  $\mathbf{h}_n$  is the field difference on the two sublattices.  $\alpha_m$  and  $\alpha_n$  are the damping coefficients associated with the motion of  $\mathbf{m}$  and  $\mathbf{n}$ , which can be determined from the first-principles theory [29].

To the first order in  $\mathbf{m}$ , one can decouple the motion from Eq. (3) and obtain,

$$\mathbf{n} \times [\partial_{tt} \mathbf{n} + a\alpha \partial_t \mathbf{n} + \mathbf{T}_s + \mathbf{T}_d] = 0, \quad (4)$$

where  $\mathbf{T}_s \equiv -a(A - L^2/a)\partial_{zz}\mathbf{n} - (aK - h^2)n_z\hat{\mathbf{z}}$ ,  $\mathbf{T}_d \equiv 2L\partial_z\mathbf{n} \times \partial_t\mathbf{n} + \mathbf{h} \times \partial_t\mathbf{n} - L\partial_z\mathbf{h} + a\mathbf{g}$ , and  $\alpha \equiv \alpha_n$ . Note that for the motion of wide DWs, the  $\alpha_m$  term can be neglected [30], even though its value can be significantly larger than  $\alpha_n$ .

*AFM domain wall.*— First of all, the static DW profile can be obtained by setting  $\partial_t \mathbf{n} = 0$  in Eq. (4). In spherical coordinates, we denote  $\mathbf{n} = (\sin\theta \cos\phi, \sin\theta \sin\phi, \cos\theta)$ . Similar to the ferromagnetic counterpart [31], we apply the following DW ansatz:

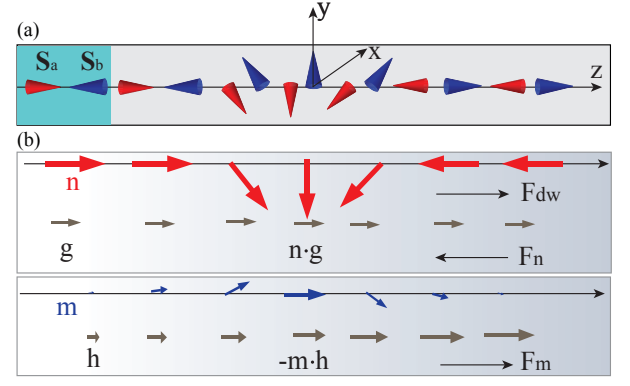


FIG. 1. (Color online)(a) Schematics of a two-sublattice AFM nanowire with a head-to-head  $180^\circ$  domain wall. (b) Schematics of a spatial distribution of Néel order  $\mathbf{n}$  (red arrow) and magnetization order  $\mathbf{m}$  (blue arrow) of a  $180^\circ$  DW. The directions of the three driven forces are also indicated as thin arrows.

$\theta = 2 \tan^{-1} \{ \exp[(z - z_c)/\Delta] \}$ , where  $z_c$  is the DW center and  $\Delta$  the DW width. For a uniform field ( $\mathbf{g} = 0$ ), the solution is,

$$\Delta = \Delta_0 / (1 - h^2/aK)^{1/2}, \quad (5)$$

where  $\Delta_0 \equiv \sqrt{A/2K}$  is the DW width in the absence of the external field. Therefore, the DW width increases with the applied field, but breaks down at the critical field  $h_c = \sqrt{aK}$ .

Next, for a propagating DW, we apply the ansatz of  $\mathbf{n} = \mathbf{n}(z - vt)$ , where  $v = \partial_t z_c$  is the velocity of DWs. From the vector product,  $\partial_z \mathbf{n} \times \text{Eq. (4)}$ , followed by an integration over the whole space, one can obtain the Thiele equation [21, 32],

$$M_{zz}(\partial_{tt} z_c + a\alpha \partial_t z_c) = F_z, \quad (6)$$

where  $M_{zz} \equiv (1/a) \int (\partial_z \mathbf{n})^2 dz = 2/(a\Delta)$ . Here  $F_z$  is the effective driving force on the DW. We found that for any applied field, the driving force can always be decomposed into three different components, i.e.,  $F_z = F_m + F_n + F_{dw}$ , where,

$$\begin{aligned} F_m &= \frac{L}{a\Delta} \int (\partial_z h) \sin^2 \theta \, dz, \\ F_n &= -\frac{1}{\Delta} \int g \sin^2 \theta \, dz, \\ F_{dw} &= \frac{1}{2A} \int (\partial_z h^2) \sin^2 \theta \, dz. \end{aligned} \quad (7)$$

For a steady DW motion where  $\partial_{tt} z_c = 0$ , the velocity of the DW depends on the relative sizes of these forces,

$$v = (\Delta/2\alpha) (F_m + F_n + F_{dw}). \quad (8)$$

As a result, the propagation direction of the DW depends on the relative sizes of the force components. In other

words, the velocity can be symmetric, anti-symmetric and asymmetric, depending on the spatial profile of the applied field; this framework can be applied to understand the conflicting results between Ref [12] and [28].

To elaborate further, let us now discuss the physical origins of these three forces. First,  $F_m$  comes from the net magnetization of a DW originated from the parity-breaking term ( $L$ ). This net magnetization interacts with the external field, and can sense the average magnetic field gradient. As a result, the DW tends to move to the high field region to reduce the total Zeeman energy  $-\mathbf{m} \cdot \mathbf{h}$ , i.e. to the direction of  $\partial h / \partial z > 0$ , as shown in the bottom panel of Fig. 1(b). Second,  $F_n$  is proportional to the average field difference on the two sublattices, arising from the spatial variation of the magnetic field. It plays the role of a Néel field [33] that couples to the Néel order as indicated by the term of  $\mathbf{n} \cdot \mathbf{g}$  in Eq (2). For a continuous monotonic spatially varying field,  $F_n$  is related to the field derivative and has an opposite sign to  $F_m$ . This force tends to drive a DW to move along the direction of  $\partial h / \partial z < 0$ . Finally, the force  $F_{dw}$  is referred to as the “field-dependent DW energy effect”, based on the fact that  $K$  is modulated by a factor  $1 - h^2 / aK$  as shown in the DW width given by Eq. (5). A DW tends to move to the direction with smaller anisotropy i.e. larger  $h^2$  region, to reduce the total free energy. Therefore the reversal of the field direction does not change the direction of DW motion.

*Examples.*— Next, we shall show that the effects of the three forces can be manifested independently, by considering three different types of inhomogeneous external fields, namely,

$$\begin{aligned} \text{Linear} : H_i &= H_0 \frac{i}{2N}, (i = 0, 1, \dots, 2N - 1) \\ \text{Stair} : H_{2i} &= H_{2i+1} = H_0 \frac{i}{N}, (i = 0, 1, \dots, N - 1) \\ \text{Rectangular} : H_{2i} &= 0, H_{2i+1} = \frac{H_0}{2N}, (i = 0, 1, \dots, N - 1) \end{aligned} \quad (9)$$

where  $2N$  is the total number of spins and  $H_0$  characterizes the field inhomogeneity. For the linear field, the  $F_{dw}$  term dominates the DW motion, which means that the velocity does not change if the applied field is reversed. It is because  $L/A = d/2$ ,  $g = d\partial_z h/2$ , the first two forces cancel each other, i.e.,  $F_m = -F_n$ . In this case, the velocity in Eq. (8) can be approximated [34] by  $v \approx \Delta^2 H_0^2 / (2a\alpha N)$ , which is shown with the blue line in Fig. 2(a). The value is normally very small (order of tens meter per second at most) for a typical field gradient of  $1 \text{ T}/\mu\text{m}$ . For the stair field,  $F_n = 0$  and  $F_m$  dominates the DW motion. In the weak field regime  $H_0 \ll L/\Delta$ ,  $F_{dw}$  gives a second order correction to the velocity and thus we have  $v = L\Delta H_0 / (a\alpha N) + \Delta^2 H_0^2 / (a\alpha N)$ , which is shown by the black line in Fig. 2(a). Here the moving direction of DW is reversed when the field is reversed. Note that the magnitude of the velocity is asymmetric to

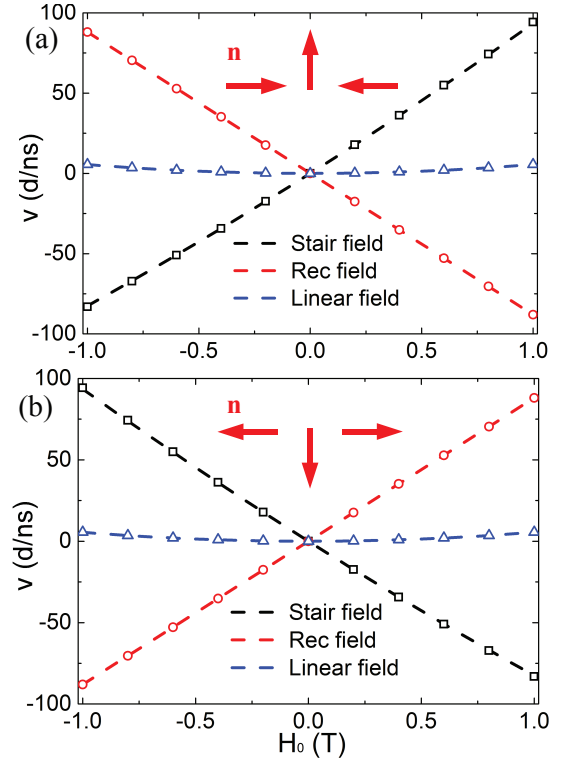


FIG. 2. (Color online) Velocity of a head-to-head DW (a) and a tail-to-tail DW (b) as a function of field strength for the linear (triangles), stair (squares) and rectangle (circles) fields, respectively. The dashed lines are theoretical prediction Eq. (8). The model parameters are  $N = 10^3$ ,  $J = 16 \text{ meV}$ ,  $K = 0.02 \text{ meV}$ ,  $S = 1$  and  $\alpha = 0.02$ .

the external field due to the contribution from  $F_{dw}$ .

For the rectangular field,  $F_n$  dominates DW motion because  $F_m = 0$ . The DW velocity is  $v = \Delta H_0 / (\alpha N)$ , as shown with the red line in Fig. 2(a). In this case, the moving direction is reversed as the field reverses. Moreover, a tail-to-tail DW moves in the opposite direction to that of a head-to-head DW under stair and rectangle fields while the moving direction does not depend on DW types under linear fields, as shown in Fig. 2(b). This feature can be readily explained by analyzing the direction of the three forces.

To verify our analytical results for the three scenarios, we performed numerical simulations of coupled Landau-Lifshitz-Gilbert (LLG) equations for the two sublattice spins,  $\partial_t \mathbf{S}_i = -\mathbf{S}_i \times \mathbf{H}_{\text{eff}} + (\alpha/S) \mathbf{S}_i \times \partial_t \mathbf{S}_i$ , where  $\alpha$  is the Gilbert damping and  $\mathbf{H}_{\text{eff}}$  is the effective field given by  $\mathbf{H}_{\text{eff}} = -(\delta \mathcal{H} / \delta \mathbf{S}_i)$ . In Fig. 2, the black rectangles, red circles and blue triangles represent the field dependence of DW velocity for linear, stair, and rectangular fields, respectively. It is shown that the theoretical predictions [Eq. (8)] agree very well with the numerical simulations.

*High-speed DW on synthetic AFMs*— Within this framework of classifying the forces on AFMs, we are now ready to discuss how an AFM DW can be manipulated

efficiently. According to above analysis, it is clear that the quadratic force  $F_{dw}$  is only a second-order effect for a weak field, and  $F_m$  is proportional to the gradient of average magnetic field that is normally not very large. Therefore, in order to achieve a high DW velocity, one can instead consider strengthening the inter-sublattice force  $F_n$ , i.e., with a large average-field difference on the two sublattices.

Specifically, we predict that a strong inter-sublattice force can be achieved readily in a synthetic antiferromagnet (SAFM) [35, 36], which consists two antiferromagnetically coupled ferromagnetic chains (see Fig. 3(a)). When the inter-chain coupling is much stronger than the intra-chain exchange coupling, this system is equivalent to a one-dimensional antiferromagnet, where the atoms on the top and bottom chains correspond to the sublattices  $a$  and  $b$ , respectively. If a uniform field is applied in the top/bottom chain, its effect corresponds to a rectangle field applied in the two sublattices, and this could effectively drive the coupled DW to move.

As shown in Fig. 3(b), our numerical simulations show that DW velocity increases with the field, and reaches a value of 17d/ps (around 10 km/s) for a 0.5 T field. This is almost one order of magnitude larger than the velocity of electric-current-driven DW motion (0.75 km/s) [37]. For a comparison, the DW velocity in the system without inter-layer AFM coupling is shown as the dashed lines and it is almost three orders of magnitude smaller than the velocity in a SAFM. This is because the velocity is given by,  $v_{FM} = H\Delta(\alpha + 1/\alpha) \approx H\Delta\alpha$  [40], while the velocity in an SAFM is scaled by a factor of  $1/\alpha$ . Given that  $\alpha \ll 1$ , the DW can move much faster in a SAFM.

Therefore, the synthetic antiferromagnet is a promising system for the high DW velocity of around 10 km/s in a uniform field in one of the ferromagnetic layers. This mechanism should work for metals, insulators, and semiconductors. The driving field can be the Oersted field generated from an electric current. Alternatively, the spin-orbit field in the two antiferromagnetically coupled ferromagnetic layer sandwiched by a non-magnetic layer also takes opposite signs at the two interfaces and thus can be used to induce fast DW motion.

*Discussions and Conclusions.*— Finally, let us compare our results with the conflicting theoretical predictions in the literature. If the net magnetization dominates the DW motion, then the DW propagation indeed reverses its direction as the field direction is reversed. The simulation results in literature [28], based on the dynamic equations of  $\mathbf{m}$  and  $\mathbf{n}$ , did not include the Néel field term of  $\mathbf{n} \cdot \mathbf{g}$ . In fact, their “linear field” corresponds to our stair field; the DW propagating direction should reverse as the field direction is reversed. However, if the linear field is considered in a Heisenberg model, the DW velocity should be symmetric with respect to the field, since  $F_m$  and  $F_n$  cancel each other and the dominate driven force is DW energy, which depends quadratically

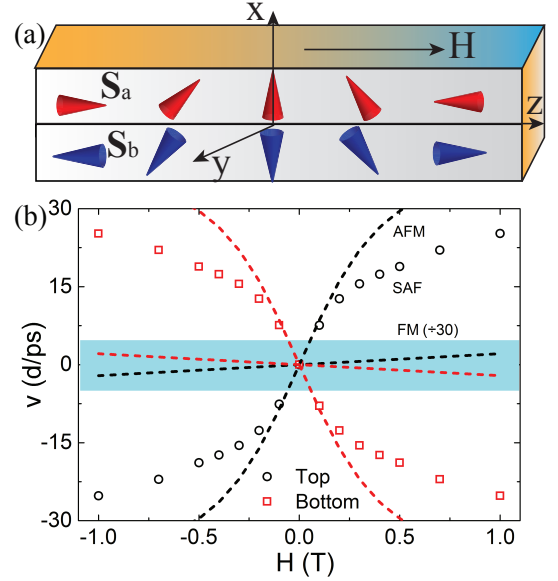


FIG. 3. (Color online) (a) Schematic illustration of a synthetic antiferromagnet consists of two ferromagnetic chains with an antiferromagnetic inter-chain coupling. (b) Simulation results of DW velocity as a function of the applied field. The dashed line labelled with AFM is for a traditional two-sublattice a synthetic AFM under a rectangle field while the dashed line labelled with FM is for a single ferromagnetic chain. The  $\div 30$  sign means that the real DW velocity is  $1/30$  of the plot. The intra-layer and inter-layer exchange coupling are  $J_1 = -16$  meV and  $J_2 = 16$  meV, respectively.  $K = 0.02$  meV,  $\alpha = 0.02$ .

on magnetic fields. These observations are well justified by our atomistic numerical simulations.

Furthermore, we note that the quadratic field-dependence of DW energy is fundamentally different from previous quadratic-field term from the interaction between the external field with its induced magnetization [12]. In an AFM, the magnetic susceptibility is zero or vanishingly small when the temperature is far below the Néel temperature and the field is smaller than the spin-flop field [38, 39]. Thus the effect caused by the induced magnetization should not play an important role in DW motion.

In conclusion, we provided a framework for studying AFM DW motion under the spatial inhomogeneous magnetic fields, where any applied field can be decomposed into three different force components, for driving an AFM DW. The three force components are respectively originated from the net DW magnetization that interacts with an averaged field over the neighboring unit-cells, the field difference on the two sublattices that couples to the Néel order and plays a role of the Néel field, and quadratic field dependence of DW energy due to the non-collinear DW spin structure. The first two forces tend to cancel each other for a linear field. The third force can drive a DW move at a speed that is insensitive to both DW



types and field direction. To produce a high-speed DW motion, rectangular or stair field is favorable for taking the advantage of the second force. Finally, supported by numerical simulations, we predicted that SAFM can become a promising candidate for realizing this proposal.

*Acknowledgments.*— We acknowledge the financial support from National Natural Science Foundation of China (NSFC) Grants (Nos. 61704071 and 11604169). MHY acknowledges support by NSFC Grant (No. 11405093), Guangdong Innovative and Entrepreneurial Research Team Program (2016ZT06D348), and Science, Technology and Innovation Commission of Shenzhen Municipality (ZDSYS20170303165926217 and JCYJ20170412152620376). XRW was supported by the NSFC Grant (No. 11774296) as well as Hong Kong RGC Grants (Nos. 16300117 and 16301816).

---

\* These authors contributed equally to this work.

† Electronic address: yung@sustc.edu.cn

‡ Electronic address: phxwan@ust.hk

- [1] A. V. Kimel, A. Kirilyuk, A. Tsvetkov, R. V. Pisarev, and Th. Rasing, *Nature*(London) **429**, 850 (2004).
- [2] R. A. Duine, P. M. Haney, A. S. Nunez, and A. H. MacDonald, *Phys. Rev. B* **75**, 014433 (2007).
- [3] P. M. Haney and A. H. MacDonald, *Phys. Rev. Lett.* **100**, 196801 (2008).
- [4] Y. Xu, S. Wang, and K. Xia, *Phys. Rev. Lett.* **100**, 226602 (2008).
- [5] T. Kampfrath, A. Sell, G. Klatt, A. Pashkin, S. Mährlein, T. Dekorsy, M. Wolf, M. Fiebig, A. Leitenstorfer, and R. Huber, *Nat. Photon.* **5**, 31 (2010).
- [6] A. H. MacDonald and M. Tsoi, *Philos. Trans. R. Soc. A* **269**, 3098 (2011).
- [7] K. M. D. Hals, Y. Tserkovnyak, and A. Brataas, *Phys. Rev. Lett.* **106**, 107206 (2011).
- [8] E. G. Tveten, A. Qaiumzadeh, O. A. Tretiakov, and A. Brataas, *Phys. Rev. Lett.* **110**, 127208 (2013).
- [9] R. Cheng, J. Xiao, Q. Niu, and A. Brataas, *Phys. Rev. Lett.* **113**, 057601 (2014).
- [10] X. Marti et al., *Nat. Mater.* **13**, 367 (2014).
- [11] P. Wadley et al., *Science* **351**, 587 (2016).
- [12] O. Gomonay, T. Jungwirth, and J. Sinova, *Phys. Rev. Lett.* **117**, 017202 (2016).
- [13] T. Shiino, S. H. Oh, P. M. Haney, S. -W. Lee, G. Go, B. -G. Park, and K. -J. Lee, *Phys. Rev. Lett.* **117**, 087203 (2016).
- [14] S. Selzer, U. Atxitia, U. Ritzmann, D. Hinzke, and U. Nowak, *Phys. Rev. Lett.* **117**, 107201 (2016).
- [15] T. Jungwirth, X. Marti, P. Wadley, and J. Wunderlich, *Nat. Nanotech.* **11**, 231 (2016).
- [16] X. Zhang, Y. Zhou, and M. Ezawa, *Sci. Rep.* **6**, 24795 (2016).
- [17] J. Barker and O. A. Tretiakov, *Phys. Rev. Lett.* **116**, 147203 (2016).
- [18] S. Fukami, C. Zhang, S. Dutta Gupta, A. Kurenkov, and H. Ohno, *Nat. Mater.* **15**, 535 (2016).
- [19] H. Y. Yuan and X. R. Wang, *Appl. Phys. Lett.* **110**, 082403 (2017).
- [20] W. Wang, C. Gu, Y. Zhou, and H. Fangohr, *Phys. Rev. B* **96**, 024430 (2017).
- [21] E. G. Tveten, A. Qaiumzadeh, and A. Brataas, *Phys. Rev. Lett.* **112**, 147204 (2014).
- [22] S. Takei, B. I. Halperin, A. Yacoby, and Y. Tserkovnyak, *Phys. Rev. B* **90**, 094408 (2014).
- [23] H. Y. Yuan and M.-H. Yung, preprint at arXiv:1711.04394
- [24] S. M. Wu et al., *Phys. Rev. Lett.* **116**, 097204 (2016).
- [25] F. Schlickeiser, U. Ritzmann, D. Hinzke, and U. Nowak, *Phys. Rev. Lett.* **113**, 097201 (2014).
- [26] X. S. Wang and X. R. Wang, *Phys. Rev. B* **90**, 014414 (2014).
- [27] P. Yan, Y. Cao, and J. Sinova, **92**, 100408(R) (2015).
- [28] E. G. Tveten, T. Muller, J. Linder, and A. Brataas, *Phys. Rev. B* **93**, 104408 (2016).
- [29] Q. Liu, H. Y. Yuan, K. Xia, and Z. Yuan, *Phys. Rev. Mater.* **1**, 061401(R) (2017).
- [30] H. Y. Yuan, Q. Liu, K. Xia, Z. Yuan and X. R. Wang (unpublished).
- [31] H. Y. Yuan, Z. Yuan, K. Xia, and X. R. Wang, *Phys. Rev. B* **94**, 064415 (2016).
- [32] A. A. Thiele, *Phys. Rev. Lett.* **30**, 230 (1972).
- [33] J. Železný, H. Gao, K. Výborný, J. Zemen, J. Mašek, A. Manchon, J. Wunderlich, J. Sinova, and T. Jungwirth, *Phys. Rev. Lett.* **113**, 157201 (2014).
- [34] The domain wall velocity is averaged on the first 1 ns. Since the domain wall speed is very small in this period, we assume that the domain wall center is close to its initial position such that the integral in  $F_{dw}$  can be calculated analytically to derive the DW velocity.
- [35] S. S. P. Parkin, N. More, and K. P. Roche, *Phys. Rev. Lett.* **64**, 2304 (1990).
- [36] W. R. Bennett, W. Schwarzacher, and W. F. Egelhoff, *Phys. Rev. Lett.* **65**, 3169 (1990).
- [37] S. -H. Yang, K. -S. Ryu, and S. Parkin, *Nat. Nanotech.* **10**, 221 (2015).
- [38] C. Trapp and J. W. Stout, *Phys. Rev. Lett.* **10**, 157 (1962).
- [39] J. M. D. Coey, *Magnetism and Magnetic Materials*, Cambridge University Press (New York, 2010)
- [40] R. Wieser, E. Y. Vedmedenko, and R. Wiesendanger, *Phys. Rev. B* **81**, 024405 (2010).